BigBOSS: A stage IV dark energy redshift survey

Michael J. Sholl[1], Mark R. Ackerman[2], Chris Bebek[3], Robert Besuner[1], Arjun Dey[4], Jerry Edelstein[1], Patrick Jelinsky[1], Michael L. Lampton[1], Michael E. Levi[3], Ming Liang[4], Paul Perry[3], Natalie Roe[3], Joseph Silber[3], David Schlegel[3]

[1]University of California at Berkeley Space Sciences Laboratory, Berkeley CA
[2]University of New Mexico, Albuquerque, NM
[3]Lawrence Berkeley National Laboratory, Berkeley CA
[4]National Optical Astronomy Observatory, Tucson AZ

ABSTRACT

BigBOSS is a Stage IV dark energy experiment based on proven techniques to study baryon acoustic oscillations and the growth of large scale structure. The 2010 Astronomy and Astrophysics Decadal Survey labeled dark energy as a key area of exploration. BigBOSS is designed to perform a 14,000 square degree survey of 20 million galaxies and quasi-stellar objects. The project involves installation of a new instrument on the Mayall 4m telescope, operated by the National Optical Astronomy Observatory. The instrument includes a new optical widefield corrector, a 5,000 fiber actuator system, and a multi-object spectrometer. Systems engineering flowdown from data set requirements to instrument requirements are discussed, along with the trade considerations and a pre-conceptual baseline design of the widefield optical corrector, spectrometer and fiber positioner systems.

Keywords: dark energy, widefield imaging, widefield corrector, optomechanics
Contact: mike.sholl@ssl.berkeley.edu

1. THE BIGBOSS EXPERIMENT & SURVEY REQUIREMENTS

BigBOSS is an instrument planned for installation on the existing 4m Mayall telescope at Kitt Peak. The instrument consists of a new prime focus corrector, 5,000 robotically controlled fiber positioners, a fiber system[1] and a set of 10 spectrometers[2]. Level 1 scientific requirements and goals of the survey are discussed by Schlegel et al. detail in[3,4] and by Mostek et al.[5] at this conference, and are not repeated herein. Derived Level 2 data set requirements describe observational needs of the survey and are listed in Table 1.

Table 1: Level 2 data set requirements describe the goals of the survey.

Parameter	Requirement
Survey area	14,000 square degrees
Redshift range	Luminous Red Galaxies (LRG): $0.5 < z < 1.0$ Emission Line Galaxies (ELG): $0.5 < z < 1.6$ Quasi-stellar objects (QSOs): $0.5 < z < 3.5$, Ly-α QSOs: $2.2 < z < 3.5$
Galaxy dN/dV	$> 1\times10^{-4}$ (h/Mpc)^3
Number of redshifts	20×10^6
Redshift accuracy	$\sigma_z < 0.001(1+z)$ rms < 5% catastrophic failures, Resolve [OII] doublet for $0.76 < z < 1.6$

The instrument spans a wavelength range of 360–980 nm. The blue cutoff is driven by the requirement to detect emission from Ly-α QSOs at redshifts above z=2.2. Cutoff at the red end allows detection of the [OII] doublet emission lines (372.7nm and 372.9nm, rest frame) from an ELG at redshift z=1.7. Luminous red galaxies will be detected up to redshift z=1.0 using a break feature at 4000Å.

Level 2 Data Set Requirements flow down to Level 3 Instrument Requirements, which specify the field of view (FOV), number of fibers and the survey duration (500 nights). Corrector design and performance parameters are driven by the need to inject the full 360 nm to 080 nm band into a fiber, at nearly normal incidence. Point spread function (PSF) shape is important only for fiber injection efficiency, and is one of many parameters constrained to increase signal to noise. The prime focus variant was chosen for lower cost, improved stray light performance and simplified interfaces between the Mayall 4m telescope and the BigBOSS instrument. The relatively wide band (360-980 nm), and spectral resolving power required to resolve the [OII] doublet led to a three-channel spectrometer design. The spectrometer topology was driven by a need to maximize the number of fibers located on each slit. Spectrometers currently have an *f*/4 input and are discussed in Jelinsky[2]. Level 3 Instrument Requirements are detailed in Table 2.

Table 2: Level 3 Instrument Requirements

Parameter	**Requirement**
Survey duration	Complete in less than 500 nights
Instrument compatibility	Compatible with Mayall 4m telescope, preserve existing *f*/8 M2 capability
Number of fibers	5,000
Operational overhead (reposition, settle, readout CCDs)	60 s/exposure
Spectral range and resolution	360 nm < λ < 555 nm: R > 1,500 555 nm < λ < 656 nm: R > 4,000 656 nm < λ < 980 nm: R > 4,000
Optical throughput	Specified versus λ, maximize across band
Fiber positioning error (actuators, guiding, tracking, target astrometry)	1-σ error < 0.35 arcsec

2. CORRECTOR TOPOLOGY TRADES AND BASELINE DESIGN

The Mayall 4m telescope has a primary focal ratio of *f*/2.81. For reasons that will be discussed in the next two sections, magnification to *f*/4.5 helps the survey rate by allowing a reasonable spectrometer focal ratio and low-risk actuators. Terebizh[6] proposed an impressive all-spherical 3° FOV prime focus corrector for the Mayall's twin, Blanco (CTIO). This design (called *T* by Terebizh) worked over a band from 320 nm to 1100 nm at an (essentially unmagnified) focal ratio of 2.92. Geometric blur radii were from 0.26" to 0.94" (" implies arcsec). The *T* design, with spheres,

was not designed to feed a fiber system. The chief rays are not oriented normal to the local focal surface.

A 2.2˚ FOV corrector (Kent[7], et al.) was developed for Blanco and adopted for the filtered imager of the Dark Energy Survey (DES) project. It was fabricated and is currently undergoing commissioning at CTIO. DES works with five filter bands, U, G, R, I, Z, and the corrector designed to correct only over individual filter bands, not the entire spectrum simultaneously. The DES corrector is also essentially unmagnified.

One major difficulty of the design of a corrector for a broadband multi-object spectrometer is the required wide bandpass. An unmagnified corrector (such as the Terebizh *T* or DES corrector) introduces minimal lateral color. To magnify from *f*/2.81 to *f*/4.5 requires chromatic correction in the corrector design. This typically involves introducing a high-dispersion glass as an optically-powered element. Because our 5000 targets per field will have important spectral features over our the 360 nm to 980 nm wavelength range, we must correct the entire field for the entire waveband. For these reasons, a broadband magnifying corrector presents challenges beyond those encountered with a filtered, non-magnifying corrector.

Numerous advantages are realized by magnifying the *f*/2.81 primary focal ratio to *f*/4.5, and this baseline was chosen for BigBOSS. An *f*/2.81 system has mechanical tolerances roughly twice as difficult to achieve as those of an *f*/4 system. Additionally, the fiber core size required for optimal signal to noise is roughly 75 μm diameter. Actuator lateral and focus tolerances of the are much tighter than achieved by existing and proven actuators, such as the fiber positioning devices on LAMOST, developed by the University of Science and Technology China (USTC). With current-generation actuators, a 75 μm fiber would have excessive losses due to lateral misalignment.

A 5000 fiber multi-object spectrograph (MOS) at ~*f*/3 on the Mayall would require 7 mm pitch actuators. The actuators implemented successfully on the 4000 fiber LAMOST design are geared stepping motors in a theta-theta configuration[8], with a pitch of 25.6 mm. Prototypes are currently working with a 12 mm pitch, but no heritage stepping motor designs have been built successfully to date at a pitch lower than 12 mm. The current 12 mm pitch USTC design is considered low risk, because the design is similar to that of LAMOST, and prototypes have been tested successfully. Placement of 5000 actuators on a 12 mm pitch require a focal plate diameter of roughly 0.9 m. This corresponds to a 3˚ FOV at *f*/4.5 for the 3.797 m Mayall primary mirror.

Tradeoffs between Cassegrain and prime focus concepts were discussed by Ackerman[9]. The BigBOSS project is currently in an R&D phase, and has a pre-conceptual baseline optical design which is used as a yardstick for design development and trade studies. Further trades on the configuration have been performed recently[10] to optimize the design and explore alternate configurations. The baseline design has negligible vignetting (essentially only the projection of the corrector). In this design, the system pupil is located at the primary mirror. Ackerman showed that by allowing the stop to float between the primary and the corrector, and allowing ~8% variation in relative illumination from center to edge, one could reduce aberrations sufficiently to remove the second element of the corrector, thereby reducing the cost and mass of the corrector. A comparison

between the pre-conceptual baseline design and Ackerman's One Mirror Anastigmat (OMA) are listed in Table 3 and shown in Figure 1.

Table 3: Comparison between pre-conceptual baseline design and OMA.

Parameter	Pre-conceptual baseline	One Mirror Anastigmat
Lens groups	6	5
C1 diameter	1.16 m	1.15 m
Optical element mass	1400 kg	1260 kg
Vignetting at FOV edge	1%	8%
Aspheric surfaces	2	3

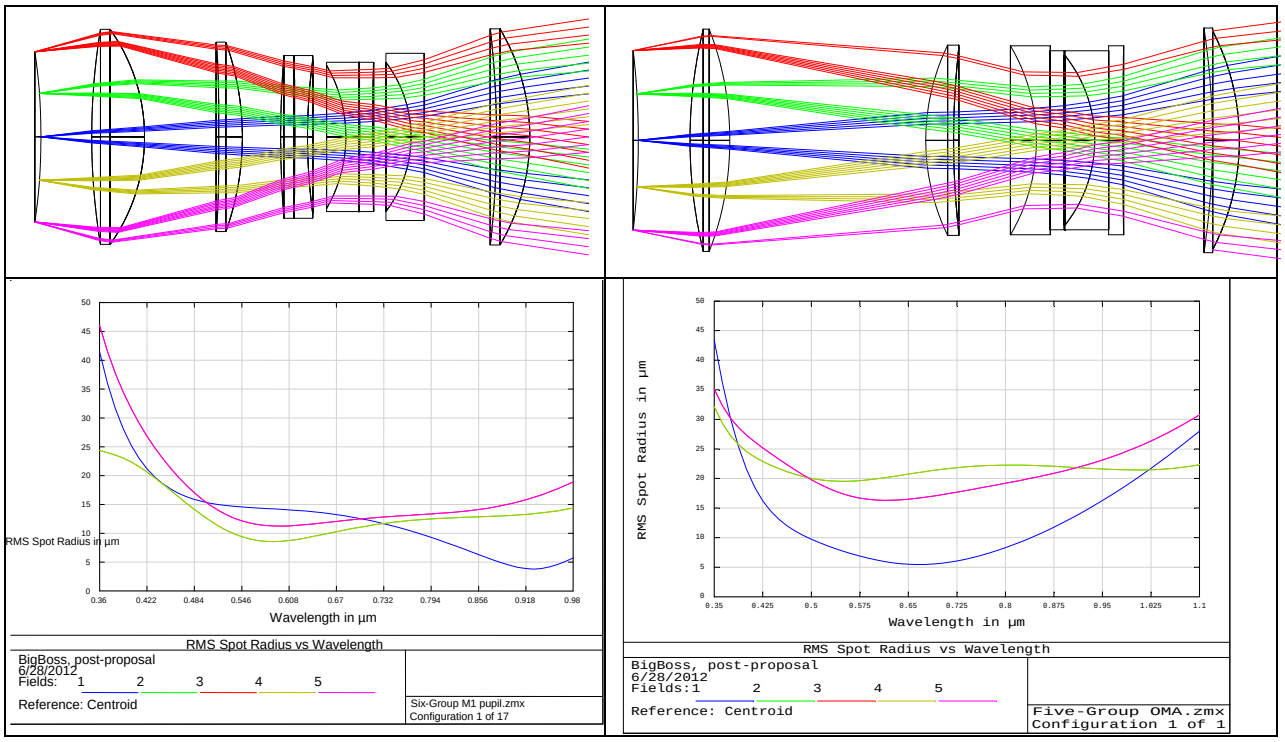

Figure 1: Comparison of six-group preconceptual baseline, and One Mirror Anastigmat corrector designs.

Current best estimates of the corrector assembly, hexapod and cage (with 25%) contingency have the mass of the BigBOSS instrument roughly the same as the existing prime focus assembly on the Mayall. The project baseline will be optimized based on the overall system throughput, cost and lead-time.

3. SPECTROMETER TRADES AND BASELINE DESIGN

The BigBOSS experiment is unique and scientifically interesting because it spans a redshift range from z = 0.5 to z = 3.5. In order to meet the Level 1 requirements, it must work to 360 nm to characterize Ly-α QSOs, at a moderate resolution of $\lambda/d\lambda$ = 1500, where $d\lambda$ is the spectral extent of the full width half maximum (FWHM) of the spectral-direction line spread function. Identification

of ELGs requires a resolving power of $\lambda/d\lambda$ = 4000 to resolve the two components of the [OII] doublet, which is the most useful spectral identifier for an ELG.

The survey rate required to complete the measurements in 500 nights, coupled with the signal to noise of the system, led to a pre-conceptual baseline architecture with 5000 repositionable fibers. While not all of these fibers will be used during exposure of a given target field, they all must be capable of simultaneous spectroscopy. Detailed discussion of the current spectrometer baseline is discussed by Jelinsky[2] at this conference. General considerations are listed in Table 4.

Table 4: Spectrometer driving parameters and ramifications

Parameter	Pre-conceptual baseline	Rationale
Number of fibers	5000	Survey rate is driven by number of targets in FOV and Poisson statistics
Telescope *f*/#	4.5	Allows *f*/4 spectrometer input
Pixels/fiber	>3	Fiber sampling
Spectrometers	10	Based on e2v and LBNL detector available size, resolving power and pixels/fiber image
Spectrometer channels	3	Driven by detector size, band, resolving power and slit size
Spectrometer input *f*/#	*f*/4	500 fibers per channel, demagnification from *f*/4 to *f*/1.8, 3.6 pixels per fiber
Telescope *f*/#	*f*/4.5	Required due to focal ratio degradation to feed an *f*/4 spectrometer

Groups of 500 fibers are placed on a single spectrometer slit. Light leaves each fiber in a roughly *f*/4 cone, is collimated, dichroically split into three channels, dispersed by a transmissive volume phase holographic (VPH) grating, then reimaged onto a charge coupled device (CCD) by a camera. Figure 2 shows this simplified, single channel transmissive spectrometer geometry. Transmissive collimators and cameras must correct chromatic aberration over the spectrometer band.

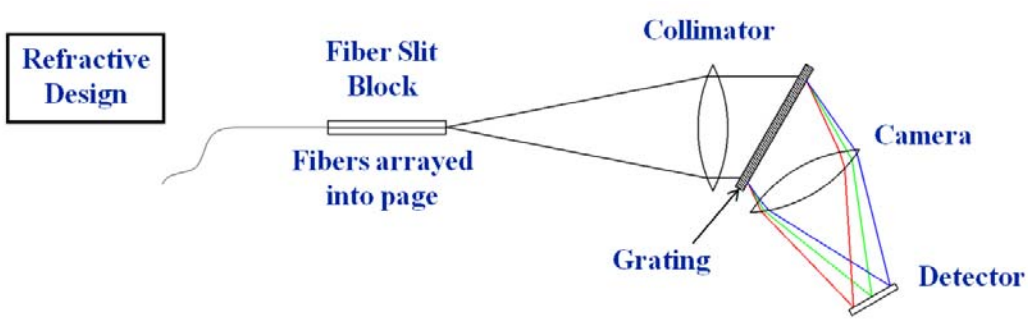

Figure 2: One arm of a standard transmissive spectrometer design is shown. Light leaves an array of fibertips, is dispersed by a grating, then focused by a camera onto a flat focal surface. System complexity is determined by the size of the fiber array relative to the system and the degree of chromatic correction required (bandpass). Transmissive designs can be made smaller than Schmidt designs due to their lack of obscurations.

Schmidt cameras may be used to eliminate chromatic aberration with a configuration based on a spherical primary mirror and a non-magnifying corrector plate. Schmidt cameras have a spherical focal surface, which may be achieved for the collimator by mounting the fibertips on a convex curved slit block. CCD detectors are flat, so the camera must have a field flattener lens, which adds complexity and some chromatic aberration.

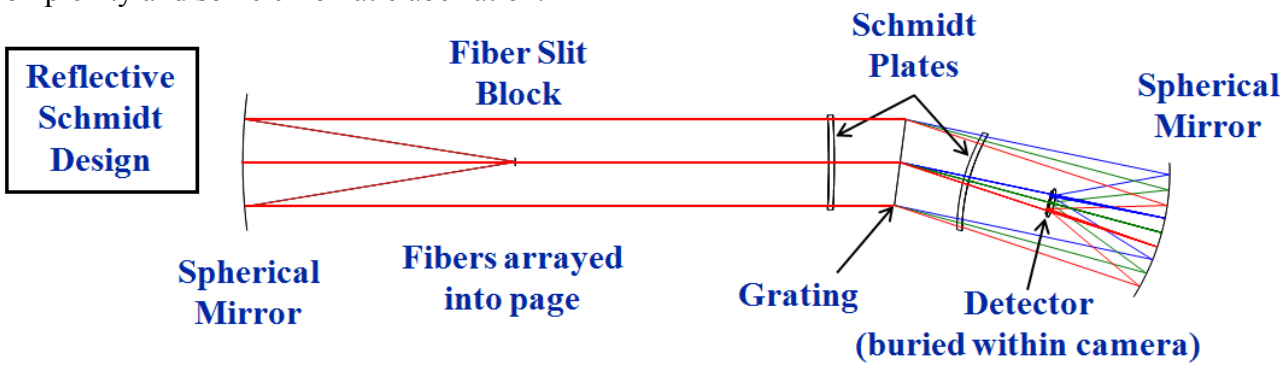

Figure 3: Spectrometer based on Schmidt collimator and Schmidt camera. Fibers are arrayed on a convex surface on the collimator. A field flattener is necessary for the camera.

The fiber slit block is in the path of the collimated beam, and therefore obstructs a rectangular region of the outgoing light. This can be minimized by suitable sizing of the fiber block, or by the use of a fold mirror (as with the Virus[11] spectrometer). The lack of chromatic aberration and simplicity of the design afford some advantages over the aforementioned transmissive design, especially with optical designs faster than *f*/4.

The obstruction of the detector and field flattener assembly degrades significantly the throughput of a Schmidt camera. To minimize light loss, the spectrometer pupil should be made as large as possible (280 mm is the current limit on the size of VPH gratings). This requires a roughly 0.5m diameter collimator and camera mirror, and still has roughly 30% light loss. The cameras require a cooled detector. As shown in Figure 4 and Figure 5, transmissive camera designs have simplified cooling relative to reflective designs, because of the easy accessibility of the detector. A reflective Schmidt camera has the detector buried within the camera. One either builds a cryostat around the detector/flattener assembly, or cools the entire Schmidt camera. For these reasons, a transmissive camera was chosen for the BigBOSS preconceptual baseline (shown in Figure 6).

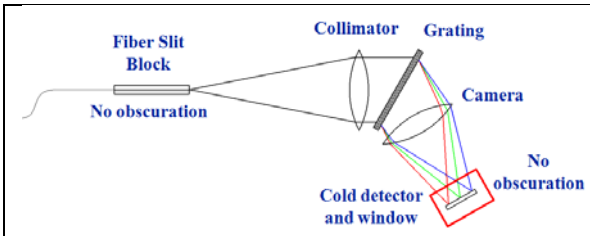

Figure 4: Refractive collimators and cameras have no obscuration. A refractive camera allows simple and local cooling of the detector.

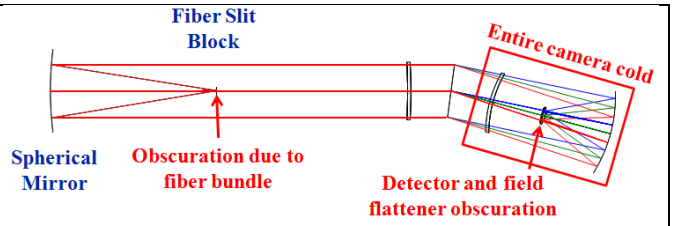

Figure 5: Reflective collimators have a small obscuration due to the fiber bundle location, while reflective cameras have significant obscuration due to the two-dimensional detector array. Cooling the detector is also difficult with a Schmidt camera, due to its interior location.

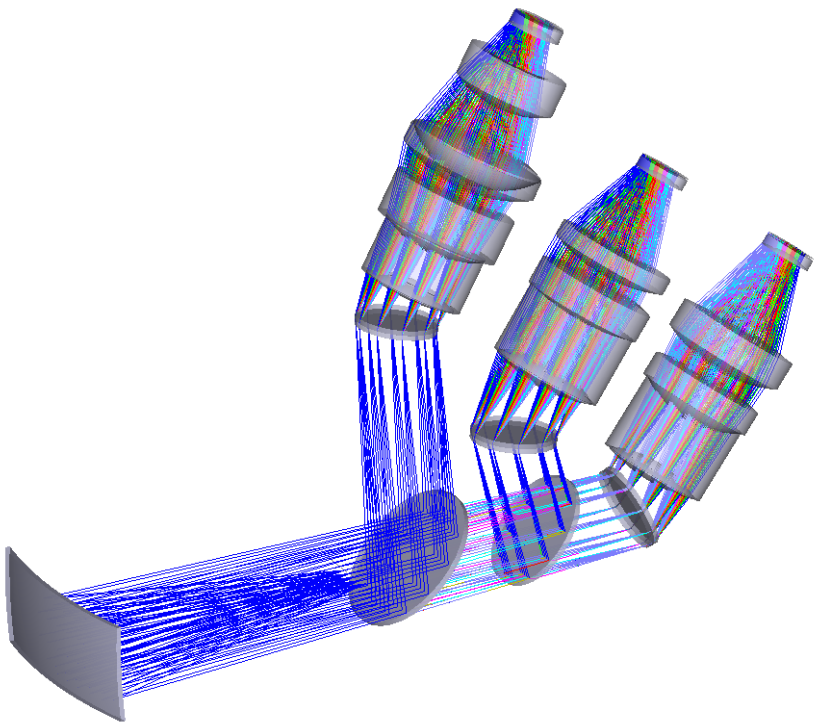

Figure 6: Preconceptual baseline spectrometer has a Schmidt collimator and three dichroic-split channels with transmissive cameras. The three arms of the spectrometer span a wavelength range of 360-980nm.

4. ACTUATOR TRADES AND BASELINE DESIGN

Selection of an actuator pitch depends not only on available actuator technology, but also the *f*/number of the spectrometer and telescope. Along with these, statistics of the target galaxy distribution on the sky suggest an optimal telescope FOV.

As stated previously, 5,000 actuators are required to complete a 14,000 sq. deg. survey in 500 nights. Observation cadence assumptions require roughly 80% of the potential targets in a given field to be observed (80% fiber efficiency). For a target density of 2,800 galaxies per square degree, the system observes 2,300. Galaxies follow a roughly Poisson distribution within a given fiber patrol radius:

$$P(n) = \frac{G^n e^{-G}}{n!}$$

in which *P(n)* is the probability that *n* galaxies lie within a patrol radius. The number of galaxies per patrol radius is denoted *G*. The patrol radius required for a 100% fill factor is:

$$R_p = \frac{FOV}{2\sqrt{N_f \times C}}$$

where N_f (5000) is the number of fibers within the FOV and *C* is a geometric factor, 0.8176. Fiber patrol radius is related to actuator pitch by the purely geometric consideration: $R_p = P_a / \sqrt{3}$. Table 5 shows the expected number of galaxies in a fiber patrol radius, based on 2,800 targets per square degree.

Table 5: Number of galaxies per positioner as a function of instrument FOV, assuming 5000 actuators.

FOV (deg)	2.0	2.2	2.5	3.0	3.5	4.0
FOV Area (deg^2)	3.14	3.80	4.91	7.07	9.62	12.57
Patrol radius R_p (arcsec)	56.3	61.9	70.4	84.5	98.6	112.7
Actuator pitch P_a (mm)	8.1	8.9	10.1	12.1	14.1	16.2
Galaxy/Positioner (G)	2.15	2.60	3.36	4.84	6.59	8.61

Given this, one can simulate the number of observations required to complete the survey for various FOVs. Table 6 shows the relative integration times required to observe the various targets, with ELGs assigned an arbitrary integration time of one. Figure 7 shows the Poisson statistics of the survey. When one target within a patrol radius is observed, it is eliminated from consideration for future observations.

Table 6: Relative integration times for galaxies and QSOs

Object	Integration time
ELG	1 time unit
LRG	2 time units
QSO	5 time units

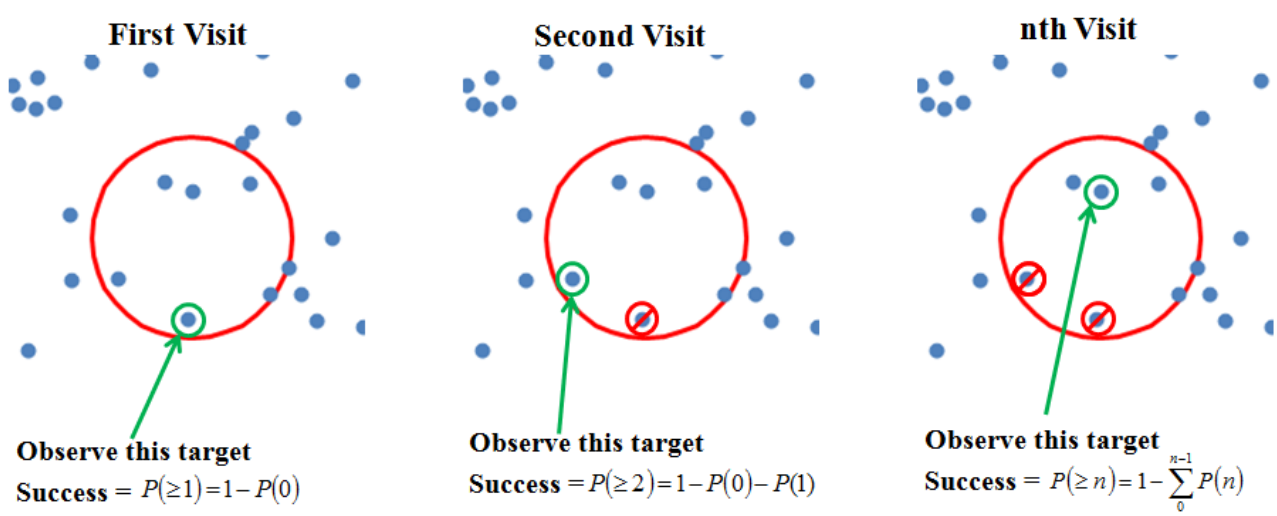

Figure 7: Target galaxies and QSOs are observed, then removed from the selection set when simulating effects of patrol radius and FOV. Statistics are based on an assumed Poisson distribution of 2,800 targets per square degree.

Figure 8 and Figure 9 show the results of the study, namely that a 3˚ FOV is optimal. Observational efficiency drops quickly below a FOV of 3˚ for a combined ELG, LRG and QSO survey. The drop occurs for smaller FOVs because fibers simply run out of targets within their smaller patrol area. Without QSOs, the increase in survey time is still present, but not as steep. Due to the Poisson statistics, a fiber efficiency of 80% can only be attained for a FOV greater than roughly 3˚. Observational efficiency of a sub-3˚ FOV survey is poor.

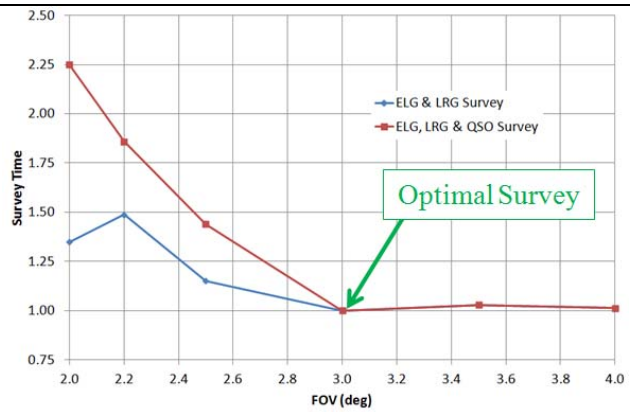

Figure 8: Below 3˚ FOV, survey time increases rapidly due to the scarcity of targets in the smaller sky area of the fiber patrol range.

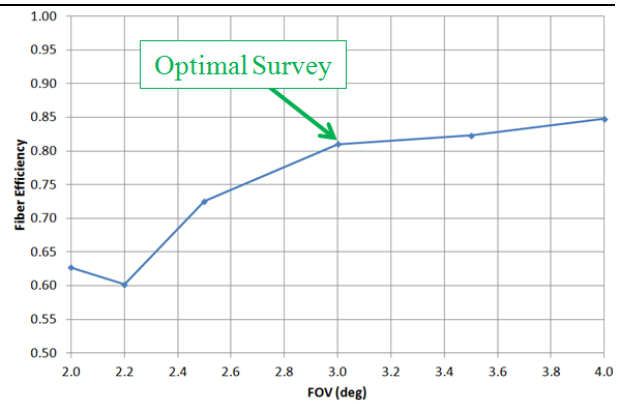

Figure 9: A fiber efficiency of 80% can be achieved for FOVs greater than 3˚.

The actuator pitch listed in Table 5 corresponding to a 3˚ FOV is ~12 mm. The actuators from LAMOST have heritage on a massively multiplexed focal array, do not tilt significantly (and lose throughput) as a function of patrol radius and are scalable to a 12 mm pitch. Although actuators with pitches smaller than 12 mm are available, they are considered high risk. For these reasons, a 12 mm pitch variant on the LAMOST actuators was selected for BigBOSS, and is in its third generation of development at USTC.

5. FOCAL PLATE AND ACTUATOR COOLING

Fiber actuators are installed in a perforated aluminum focal plate (FP) which attaches to the corrector barrel assembly. Each actuator mounts to the plate with a positive locking feature which serves as a mechanical and thermal link to the focal plate. The location of 5,000 actuators forward of the telescope pupil requires care in the thermal design. Historical records at the Mayall telescope indicate that seeing will not be spoiled if the corrector assembly external surfaces are held within 1˚C of the ambient air temperature.

Each actuator dissipates roughly 200 mW during the one minute reconfiguration period, with roughly a duty cycle of 50%. This equates to ~500 W during reconfiguration, or 25 W continuously (averaged over a night). If this heat dissipated through natural convection, seeing of the telescope would be degraded. Development of the thermal control system is a key design challenge and area of study during the R&D phase. While several concepts have been studied, and are under consideration, they all are based on an insulated thermal shroud which effectively encloses the skyward end of the FP. Figure 10 shows a view of the integrated cage and barrel assembly with the thermal fairing.

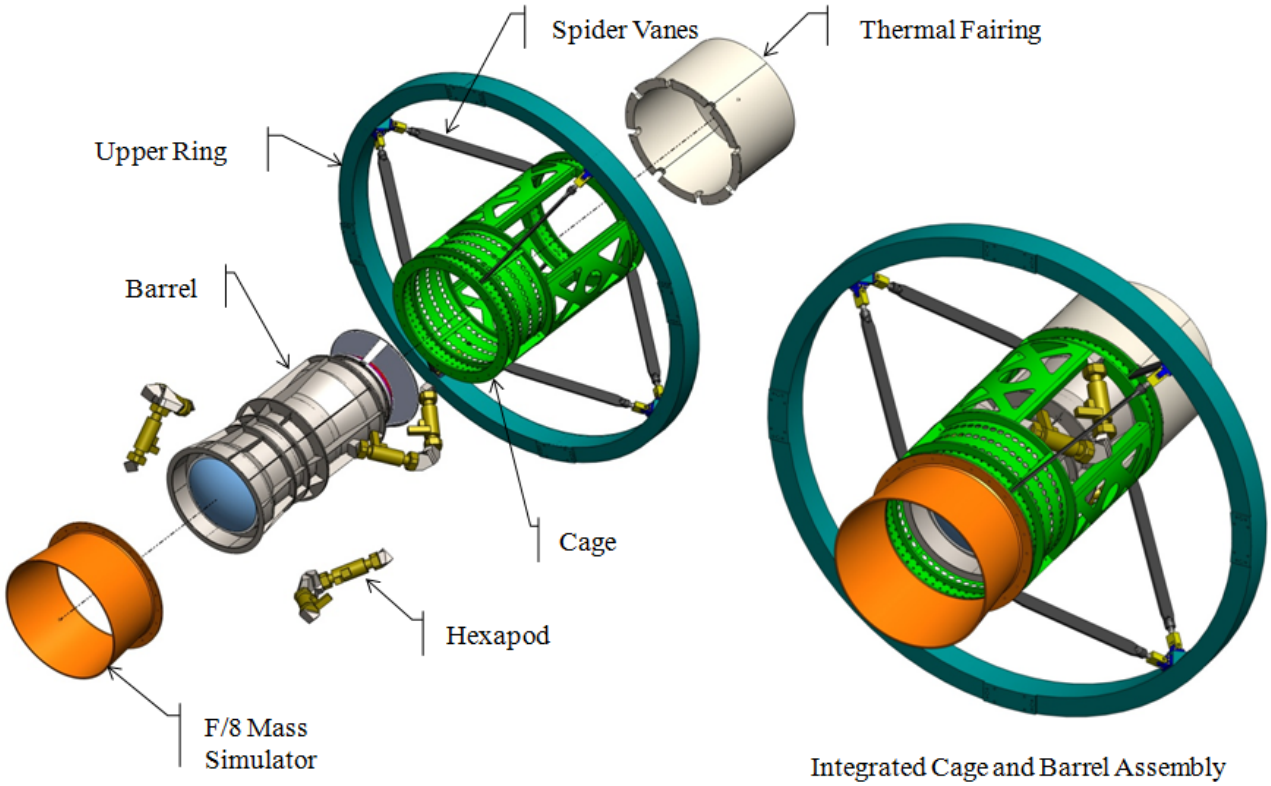

Figure 10: An insulative thermal fairing prevents heat from the fiber positioners from naturally convecting through the telescope pupil. Historical data from the Mayall telescope indicate that assemblies ahead of the telescope pupil will not contribute to seeing if they are held within one degree C of ambient.

Lateral heat transfer in the aluminum FP is hindered by the degree to which the plate is perforated. Holes of diameter 10 mm are located on a 12 mm, roughly hexagonal pitch. This leaves a minimum ligament thickness of less than 2 mm between holes (Figure 11) and leads to both decreased effective thermal conductivity and structural stiffness when compared to a solid aluminum plate. A liquid cooling system is impractical due to space limitations. The structure is marginally similar to a tube bank heat exchanger, analysis of which is described by Osweiller[12]. By passing air through the plate, either through the body of the actuator, or around a gap on its periphery, actuator waste heat is conducted readily to the fluid, and efficiently carried away from the actuator by localized forced convection (
Figure 12).

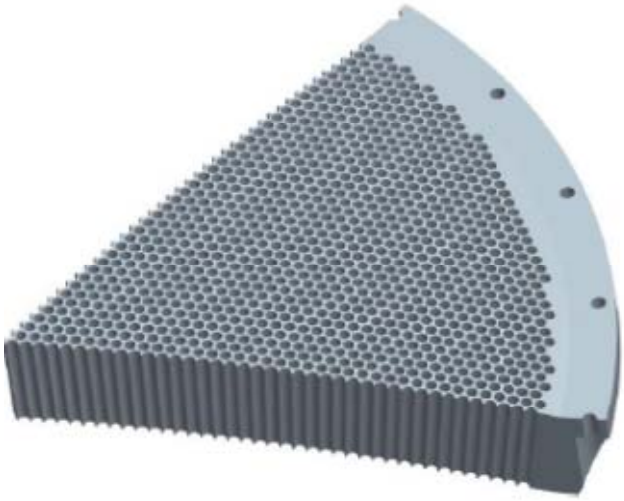

Figure 11: Holes (10 mm) are drilled into the focal plate in a 12 mm, roughly hexagonal pattern. Because little material remains, stiffness and lateral heat transfer are reduced when compared to properties of a solid aluminum slab.

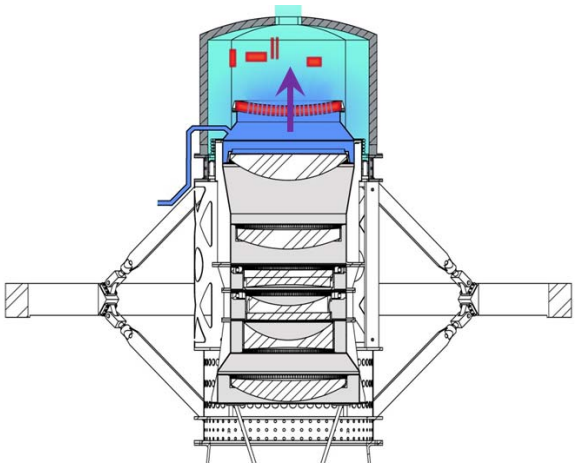

Figure 12: A 0.01 atmosphere pressure differential across the focal plate draws cooling air through a cooling channel at each actuator. All 5,000 actuators are cooled directly by localized forced convection. Waste heat is drawn away from the thermal faring by a suction line (not shown).

6. Conclusions

BigBOSS is a Stage IV dark energy experiment intended to study baryon acoustic oscillations (BAO) and the growth of large scale structure. The project involves installation of a new instrument on the Mayall 4m telescope, operated by the National Optical Astronomy Observatory. The survey is designed to perform a 14,000 square degree survey of 20 million galaxies and quasi-stellar objects. Systems flowdown from data set to instrument requirements were discussed, as well as trade studies and rationales which led to the current R&D phase preconceptual baseline designs for the prime focus corrector, spectrometer and fiber positioner system. The current pre-conceptual design with a 3˚ FOV and low-risk 12 mm pitch actuators is shown to be near-optimal.

ACKNOWLEDGMENTS

We gratefully acknowledge the support of the Director, Office of Science, U.S. Department of Energy, through contract DE-AC03-76SF 00098. Management and engineering staff at the Kitt Peak National Observatory were instrumental in defining the BigBOSS program. We also acknowledge the contributions and advice of the DES team, including (but not limited to) Brenna Flaugher, Steve Kent, Herman Cease and Tom Diehl. Robin Lafever and Christoph Schenk contributed figures.

REFERENCES

[1] Edelstein, J.E., Optical fiber systems for the BigBOSS instrument, Proc. SPIE 8450-114 (2012).
[2] Jelinksy, P., The BigBOSS Spectrograph, Proc. SPIE 8446-238 (2012).
[3] Schlegel, D., et al., BigBOSS: The Ground-Based Stage IV Dark Energy Experiment, arXiv:0904.0468 (2009).
[4] Schlegel, D., et al., The BigBOSS Experiment, arXiv:1106.1706 (2011).
[5] Mostek, N., Mapping the Universe with BigBOSS, Proc. SPIE 8446-24 (2012).
[6] Terebizh, V. Yu., A wide-field corrector at the prime focus of a Ritchey-Chrétien telescope, Astronomy Letters, Vol. 30, No. 3 (2004).
[7] Kent, S., et al., Preliminary optical design for a 2.2 degree diameter prime focus corrector for the Blanco 4 meter telescope. Proc. SPIE 6269, 626937 (2006).
[8] Hu, H., Implementary scheme of parallel controllable optical fiber positioning system for LAMOST, Proc. SPIE 6269 (2006).
[9] Sholl, M.J., 2011 BigBOSS: Enabling widefield cosmology on the Mayall telescope, Proc. SPIE 8127-12 (2011).
[10] Ackerman, M.R., Analysis of Alternate Optical Concepts for the BigBOSS spectroscopic Sky Survey, Internal report, 16 August 2011.
[11] Hill, G., et al., VIRUS: a massively replicated 33k fiber integral field spectrometer for the upgraded Hobby-Eberly Telescope, Proc. SPIE 7735 (2010).
[12] Osweiller, F., Evolution and Synthesis of the Effective Elastic Constants Concept of the Design of Tubesheets, ASME Journal of Pressure Vessel Technology, Vol. 111. (1989).